Supplementary information for

Structural basis of dual activation of cell division by the actinobacterial transcription factors WhiA and WhiB

Mirjana Lilic[1,4], Neil A. Holmes[2,4], Matthew J. Bush[2], Alexandra K. Marti[2], David A. Widdick[2], Kim C. Findlay[3], Young Joo Choi[1], Ruby Froom[1], Steven Koh[1], Mark J. Buttner[2*], and Elizabeth A. Campbell[1,5,*]

[1]Laboratory of Molecular Biophysics, The Rockefeller University, 1230 York Avenue, New York, NY 10065, USA.

[2]Department of Molecular Microbiology, and [3]Department of Cell and Developmental Biology, John Innes Centre, Norwich Research Park, Norwich NR4 7UH, UK.

[4]These authors contributed equally

[5]Lead contact: campbee@rockefeller.edu

[*]Correspondence: campbee@rockefeller.edu, mark.buttner@jic.ac.uk

This PDF file includes:

Supplementary text

Figures S1 to S6

Tables S1 to S2

SI References

Supplementary Information Text

METHODS

Structural biology software was accessed through the SBGrid consortium (1).

Protein Expression and Purification.

The *S. venezuelae* WhiB:σ^A:RbpA complex

pIJ10754, a co-expression plasmid for *S. venezuelae* WhiB and σ^A, was made using the pCDFDuet-1 backbone (Novagen) to express 6His-WhiB with Strep-tag II-σ^A. To allow co-overexpression of RbpA with WhiB and σ^A, untagged RbpA was co-expressed from a compatible construct, pIJ10757, made using the pET SUMO backbone (Invitrogen). Competent Eco BL21 (DE3) cells (Novagen) were co-transformed with pIJ10754 and pIJ10757, and cells were grown to an Optical Density (O.D.) of 0.5 at 600 nm, and induced with 1 mM isopropyl beta-D-thiogalactopyranoside (IPTG) for 16 hours (h) at 18°C. The cells were resuspended in lysis buffer (50 mM Tris pH 8.0, 500 mM NaCl, 2 mM DTT) and lysed by continuous flow through a French press (Avestin). The WhiB:σ^A:RbpA complex was first enriched by Ni^{2+}-affinity chromatography. The sample was then subjected to StrepTrap HP chromatography, and the purified WhiB:σ^A:RbpA complex was eluted with lysis buffer plus 2.5 mM desthiobiotin. The presence of the [4Fe-4S] cluster in WhiB was monitored by measuring absorbance at 420 nm. A Coomassie-stained SDS-PAGE analysis of the purified WhiB:σ^A:RbpA complex is shown in Fig. 1E.

The *S. venezuelae* σ^A:RbpA complex

pIJ10762, an overexpression plasmid for *S. venezuelae* σ^A, was made using the pCDFDuet-1 backbone (Novagen) to express Strep-tag II-σ^A. To allow co-overexpression of RbpA with σ^A, untagged RbpA was coexpressed from a compatible construct, pIJ10757, made using the pET SUMO backbone (Invitrogen). Competent *Eco* BL21 (DE3) cells (Novagen) were co-transformed with pIJ10762 and pIJ10757, and cells were grown to an Optical Density (O.D.) of 0.5 at 600 nM and induced with 1 mM isopropyl β-D-thiogalactopyranoside (IPTG) for 16 hours (h) at 18°C. The cells were resuspended in lysis buffer (50 mM Tris pH 8.0, 500 mM NaCl, 2 mM DTT) and lysed by continuous flow through a French press (Avestin). The sample from the supernatant was then subjected to StrepTrap HP chromatography, and the purified σ^A:RbpA complex was eluted with lysis buffer plus 2.5 mM desthiobiotin.

S. venezuelae WhiA

6His-WhiA was expressed from pIJ10755, made using the vector pSKB2 (a derivative of pET28b). Competent *Eco* BL21 (DE3) cells (Novagen) were used for WhiA expression. Competent cells were induced with the addition of 1 mM IPTG when the OD_{600} reached 0.6 and incubated for an additional 3 hours at 37°C. Cells were then centrifuged and pellets were lysed by continuous flow through a French press (Avestin) on ice in 300 mM NaCl, 50 mM Tris pH 8.0, and 1 mM PMSF. After centrifuging for 30 minutes, the cleared lysate was then loaded onto a 5 mL Heparin HiTrap column (Cytiva, Pittsburgh, PA) at 4°C and eluted on an AKTA FPLC with a 300 mM to 1 M NaCl gradient in 25 mM Tris, pH 8.0 buffer over 30 column volumes. The peak fraction is typically eluted at 600 mM NaCl. The peak fraction was loaded on the Ni-NTA affinity column (Cytiva, Pittsburgh, PA). The WhiA protein fraction was eluted with 250 mM imidazole, 500 mM NaCl, 25 mM Tris 8.0, and 1 mM DTT. This peak fraction was concentrated to 10 mg/ml and injected onto SD200 (HiLoad 26/600 Superdex 200) equilibrated in 20 mM Tris pH 8, 500 mM NaCl, and 2 mM DTT.

Construction of *S. venezuelae* AM1, a strain expressing the β′ subunit of RNA polymerase with a C-terminal his tag

The PCR-targeting method of Gust et al. (2, 3) was used to introduce a 3' in-frame 21-bp sequence encoding six histidine residues at the *rpoC* locus, with a downstream apramycin resistance-*oriT* cassette. The his-tagging cassette was amplified with primers rpoCfor and rpoCrev, using pIJ773 (2) as a template for the apramycin resistance-*oriT* cassette. A cosmid, PI2 J3, carrying *rpoC* near the

center of its 42 kb insert, was introduced by electroporation into *E. coli* BW25113 (4) carrying pIJ790 (2). The resulting strain was induced with arabinose to express the λ recombinase genes on pIJ790 and then the PCR his-tagging cassette was introduced by electroporation. Transformants were selected using apramycin and incorporation of the his-tagging cassette into the cosmid was confirmed first by *Pac*I digestion and then by sequencing. The *rpoC*-his derivative of PI2 J3 was introduced into *E. coli* ET12567/pUZ8002 by electroporation, permitting transfer of the cosmid into *S. venezuelae* by conjugation. Exconjugants were selected on apramycin, and multiple isolates carrying double crossovers where the his-tagging cassette had been incorporated into the chromosome and the cosmid backbone had been lost were identified by screening for kanamycin-sensitive isolates among the apramycin-resistant exconjugants. Production of his-tagged β′ subunit (RpoC) was confirmed by Western blotting using anti-his tag antibodies, and a representative isolate was named *S. venezuelae* AM1.

Purification of *S. venezuelae* RNA Polymerase

S. venezuelae core RNAP was purified from native abundance from strain AM1, which carries a C-terminal His tag on the β′ subunit. Mycelium was lysed by continuous flow French press (Avestin) in 50 mM Tris-HCl, pH 8, 1 mM EDTA, 5% (v/v) glycerol, 5 mM DTT, 1 mM protease inhibitor cocktail, 1 mM phenylmethylsulfonyl fluoride, and RNAP was precipitated from the cleared lysate by polyethyleneimine (PEI) precipitation (0.35%). The PEI pellet was washed with 10 mM Tris-HCl, pH 8, 0.5 M NaCl, 0.1 mM EDTA, 5 mM DTT, 5% (v/v) glycerol, and protein was extracted from the pellet with the same buffer but containing 1 M NaCl. Protein was precipitated overnight with 35% (w/v) ammonium sulfate and resuspended in 20 mM Tris-HCl, pH 8, 5% (v/v) glycerol, 1 M NaCl, 1 mM β-mercaptoethanol. Protein was loaded on a Ni^{2+}-affinity column (HiTrap IMAC HP, Cytiva) and eluted in 20 mM Tris-HCl, pH 8, 5% (v/v) glycerol, 0.5 M NaCl, 0.25 M imidazole. Protein was concentrated and loaded on a HiLoad 16/600 Superdex 200 column (Cytiva) equilibrated in 10 mM Tris-HCl, pH 8, 5% (v/v) glycerol, 0.1 mM EDTA, 5 mM DTT, 0.5 M NaCl, and purified core RNAP was isolated by size exclusion chromatography.

The assembly of holoenzyme

Sven holo RNAP without WhiB was formed by mixing RNAP core with 5-fold molar excess of σ^A:RbpA. *Sven* holo RNAP with WhiB was formed by mixing RNAP core with 5-fold molar excess of WhiB:σ^A:RbpA. The formed holoenzymes were purified over a Superose 6 Increase 10/300 GL column (Cytiva, Pittsburgh, PA) in gel filtration buffer (20 mM Tris-HCl pH 8.0, 500 mM NaCl, 5 mM $MgCl_2$, 2.5 mM DTT). A Coomassie-stained SDS-PAGE analysis of purified holoenzyme with WhiB:σ^A:RbpA is shown in Figure 1E. When WhiA was included, RNAP holoenzymes were mixed with a five-molar excess WhiA and incubated for 10 minutes at 37^{o}C. Holoenzymes formed in this buffer were used in the transcription assay.

In vitro Transcription Assay

Transcription assays were performed with 50 nM of *Sven* RNAP holoenzymes with σ^A:RbpA with or without WhiB and WhiA in transcription buffer [10 mM Tris HCl, pH 7.9, 50 mM K-glutamate, 10 mM, $MgCl_2$, 1 mM DTT, 5 µg/ml bovine serum albumin (BSA) and 0.1 mM EDTA]. Holoenzymes were prepared as described above and they were mixed with 200 nM WhiA when WhiA was included in the reaction. The *sepX* promoter (-70 to +30) was then added (10 nM) to the holoenzymes, and the samples were incubated for 15 min at 37 °C to allow the formation of RNAP open complex. Transcription was initiated by adding a nucleotide mixture consisting of 250 µM GpU dinucleotide (Trilink Biotechnologies, San Diego, CA), 50 µM GTP, and 1.25 µCi (15 nM)- [α-P^{32}] GTP. Each reaction was allowed to proceed for 10 min at 37 °C, and reactions were quenched by the addition of 2x stop buffer (0.5X TBE, pH 8.3, 8 M urea, 30 mM EDTA, 0.05% bromophenol blue, and 0.05% xylene cyanol). Reactions were heated to 95°C for 10 min and loaded onto a polyacrylamide gel [23% Acrylamide/Bis acrylamide (19:1), 6M urea, and 1X TBE, pH8.3]. Transcription products were visualized by using Typhoon 9400 Variable

Imager (Amersham Biosciences) and quantified using Image J (5). Quantified values were plotted in a histogram and the mean standard errors were calculated from three independent data sets.

Preparation of *Sven* RNAP/WhiA/WhiB/RbpA for cryo-EM

Sven holo RNAP with σ^A/WhiB/RbpA was formed by mixing RNAP core with 5-fold molar excess of σ^A:WhiB:RbpA. The formed holoenzymes were purified over a Superose 6 Increase 10/300 GL column (Cytiva, Pittsburgh, PA) in gel filtration buffer (20 mM Tris-HCl pH 8.0, 150 mM K-glutamate, 5 mM $MgCl_2$, 2.5 mM DTT). The eluted RNAP holoenzymes were concentrated at 5 mg/mL (12 μM) by centrifugal filtration (Amicon Ultra). RNAP holoenzymes were mixed with a 5-fold molar excess of WhiA and incubated for 10 minutes at 37°C. The *sepX* or *sepX-2* promoter fragment was added last (final concentration of 12 μM) to the samples and incubated for 15 minutes at 37°C, before cryo-EM grid preparation.

Cryo-EM grid preparation

C-flat holey carbon grids (CF-1.2/1.3-4Au, Protochips, Morrisville, NC) were glow-discharged for 20 sec before the application of 3.5 μL of the samples. OG, (n-Octyl-β-D-Glucoside, Anatrace, Maumee, OH), was added to the samples to a final 0.1% (w/v). Using a Vitrobot Mark IV (Thermo Fisher Scientific Electron Microscopy, Hillsboro, OR), grids were blotted and plunge-froze into liquid ethane with 100% chamber humidity at 22°C.

Cryo-EM data acquisition and processing

Grids were imaged using a 300 keV Titan Krios (Thermo Fisher Scientific Electron Microscopy) equipped with a K3 Summit direct electron detector (Gatan, Pleasanton, CA). Dose-fractionated movies were recorded in counting mode using Leginon (6) at a nominal pixel size of 1.083 Å over a defocus range of -1 μm to -2.5 μm. Movies were recorded with a dose rate of 30 electrons/physical pixel/s over a total exposure of 2 s (50 subframes of 0.04 s). A total of 13,474 movies were collected for the first dataset. A total of 10,745 movies were collected for the dataset with sepX-2 DNA. Dose-fractionated movies were gain-normalized, drift-corrected, summed, and dose-weighted using MotionCor2 (7). The contrast transfer function was estimated for each summed image using Patch CTF estimation in cryoSPARC2 (8). Blob picker in cryoSPARC2 was used to pick particles (no template was supplied). A total of 4,934,059 particles were picked from the first dataset, and 2,878,553 particles were picked from the dataset with sepX-2 DNA. Particles were extracted in cryoSPARC2 using a box size of 300 pixels. Ab-initio model was obtained and used as a 3D template. Four rounds of cryoSPARC2 adaptation of "random-phase 3Dclassification" (9) heterogeneous refinements (X=4) with 7 heterogeneous classes (N=7) were performed in cryoSPARC2 to curate and classify particles for the first dataset while three rounds with 6 heterogeneous classes (N=6) were performed for the second dataset with sepX-RPo-2 DNA. Curated particles from each dataset were refined in the Local CTF refinement (8) and polished in Relion (10). After polishing, particles were classified (N=4) in RELION using signal subtraction (9), with masked region around the WhiB, WhiA, alpha-CTD, and upstream DNA. Classified particles were reverted to the non-subtracted particles and refined using cryoSPARC2 Non-uniform refinement. Particles with WhiB density were combined with locally refined particles from Local (BETA) refinement performed with the same mask that was used in Relion particle subtraction. A composite map was generated in Phenix (11) from the local refinement RPo and non-uniform RPo. The RPo composite map contained 184,251 particles with a nominal resolution of 3.18 Å determined by using the gold-standard FSC 0.143 cutoff (12). The RPo-2 pipeline was performed in the same way, but particles were first subjected to the Relion particle subtraction and Relion 3D classification followed by polishing. Particles from the best class were further locally refined in Local (BETA) refinement in CS2. The RPo-2 composite map contained 118,181 particles with a nominal resolution of 3.12 Å determined by using the gold-standard FSC 0.143 cutoff (12). Local resolution calculations were generated using blocres and blocfilt commands from the Bsoft package (13) by using composite half maps.

Model building and refinement

For initial models of the complexes, the *Mtb* RNAP cryo-EM structure (PDB ID 7KIF for the RPo (14), was used to make the *Sven* model in the SWISS-MODEL (https://swissmodel.expasy.org). This model was manually fit into the cryo-EM density maps using UCSF Chimera (15) and real-space refined using PHENIX (11). For real-space refinement, rigid body refinement was followed by all-atom refinements with Ramachandran and secondary structure restraints. Refined models were inspected and modified in Coot (16). The refined models were 'shaken' by introducing random shifts to the atomic coordinates with RMSD of 0.16 Å to the final models of *Sven* RNAP RPo, 0.15 Å to the final models of *Sven* RNAP RPo-2. Shaken models were refined against the first half map and these refined models were used to calculate the FSC against the same first half maps (FSChalf1 or work), the second half maps (FSChalf2 or free) that were not used for the refinement, and combined (full) maps by using phenix.mtriage (12). The masked log file for the combined (full) maps was plotted in PRISM and the FSC 0.143 was marked on the graph. Remote 3DFSC Processing Server was used for processing Fourier shell correlations of cryoEM maps (17).

Complementation of *S. venezuelae* null mutants

The native promoter and wild-type coding sequence of *whiA* were amplified using the primer sets whiAfor + whiArev and cloned into *Kpn*I/*Hind*III-cut pIJ10770 (18) to generate pIJ10555 (*whiA*). Alleles of *whiA* carrying point mutations were generated by gene synthesis (GenScript) and cloned into *Kpn*I/*Hind*III-cut pIJ10770 to generate plasmids identical to pIJ10555 except for the intended changes. Complementation constructs were introduced into the *S. venezuelae whiA* mutant SV11 (19) by conjugation from *E. coli*.

Scanning Electron Microscopy (SEM)

Colonies were mounted on the surface of an aluminum stub with optimal cutting temperature compound (Agar Scientific Ltd, Essex, UK), plunged into liquid nitrogen slush at approximately -210°C to cryopreserve the material, and transferred to the cryostage of an Alto 2500 cryotransfer system (Gatan, Oxford, England) attached to a FEI NanoSEM 450 field emission gun scanning electron microscope (FEI Ltd, Eindhoven, The Netherlands). The surface frost was sublimated at -95°C for 3½ mins before the sample was sputter coated with platinum for 2 min at 10 mA at below -110°C. Finally, the sample was moved onto the cryostage in the main chamber of the microscope, held at approximately -130°C, and viewed at 3 kV.

Western blotting

Mycelial pellets originating from 2 mL of culture grown in MYM liquid medium were washed in ice-cold buffer (20 mM Tris pH 8.0, 5mM EDTA) and resuspended in 0.4 mL of sonication buffer (20 mM Tris pH 8.0, 5mM EDTA, 1 x EDTA-free protease inhibitors [Roche]). Samples were sonicated at 4.5-micron amplitude for 7 rounds of 15 seconds, separated by 15 seconds of rest on ice. Lysed samples were then centrifuged at 13,000 rpm for 15 minutes at 4ºC to remove cell debris. Total protein concentrations were determined by Bradford assay (Biorad) and the cleared cell lysates were diluted to a final concentration of 0.1 mg/mL before loading into a microplate (ProteinSimple #043-165), together with an anti-WhiA polyclonal antibody raised in rabbit (19) that had been diluted 1:100. WhiA levels were analyzed using a Wes automated Western Blotting machine (ProteinSimple, San Jose, CA) with the Wes-Rabbit (12 to 230 kDa) Master kit according to the manufacturer's instructions.

Bacterial Two Hybrid (BACTH)

BACTH vectors encoding the T18 domain of adenylate cyclase fused to the N terminus of genes encoding σ^A-homologs in *Streptomyces* were constructed. The *hrdA* gene was amplified using the primer pairs hrdA_BACTH_F/hrdA_BACTH_R and cloned into the pUT18C plasmid digested with *Xba*I and *Kpn*I to create the plasmid pMB493. Vectors for the *sigA/hrdB* (pIJ10922) *hrdD* (pIJ10923) genes had been previously constructed (20). Similarly, BACTH vectors encoding the T25 domain fused to the N-terminus of WhiB and a version of WhiB which has each of the four conserved cysteines substituted by alanine, were constructed. The primer pair whiB_BACTH_F/whiB_BACTH_R was used to amplify either the wild-type or variant sequence, the latter reaction using pIJ10607 as a template (21). To test interactions between proteins, *E. coli* BTH101 (F^- *cya-99 araD139 galE15 galK16 rpsL1* (Str^r) *hsdR2 mcrA1 mcrB1*) was co-transformed with the appropriate pKT25 and pUT18C fusion plasmid. β-gal assays were conducted as in previous studies (*e.g.* (22, 23)), according to standard methodology (24).

QUANTIFICATION AND STATISTICAL ANALYSIS

For calculations of Fourier shell correlations (FSC) in Figures S2B, and S2F, the FSC cutoff criterion was 0.143 and 0.5 (12). Image J was used to visualize and quantify gels. To quantify the transcription assays (Figure 1E), mean values and the standard error of the mean from at least three independent measurements were calculated. Structural biology software was accessed through the SBGrid consortium (1). The local resolution of the cryo-EM maps (Figures S2D and S2H) was estimated using blocres (13) with the following parameters: box size 15, verbose 7, sampling 1.1, and cutoff 0.5. The quantification and statistical analyses for model refinement and validation were generated using PHENIX (11).

Table S1. Cryo-EM data collection, models refinement and validation statistics

	***Sven* RPo** **PDB ID 8DY7**	***Sven* RPo-2** **PDB ID 8DY9**
Data collection and processing		
Magnification	67,000	81,000
Voltage (kV)	300	300
Electron exposure (e-/Å^2)	51.44	66
Defocus range (μm)	1-2.5	0-2.5
Pixel size (Å)	1.083	1.0825
Symmetry imposed	C1	C1
Initial particle images (no.)	4,934,059	2,878,553
Final particle images (no.)	184,251	118,181
Map resolution (Å) FSC threshold 0.143	3.18	3.12
Map resolution range (Å)	3.2-7	3.2-7
Refinement		
Initial model used (PDB code)	7KIF	7KIF
Model resolution (Å) FSC threshold 0.5	3.36	3.43
Model resolution range (Å)	3.2-7	3.2-7
Map sharpening B factor (A^2)	112.9	78.4
Model composition		
Non-hydrogen atoms	30021	31260
Protein residues	3612	3777
Nucleic acid residues	149	144
Ligands	5 (1 Mg^{2+}, 3 Zn^{2+}, 1 SF4)	5 (1 Mg^{2+}, 3 Zn^{2+}, 1 SF4)
B factors (A^2)		
Protein	50.06	80.26
Nucleic acid	254.26	145.15
Ligands	77.17	64.83
R.m.s. deviations		
Bond lengths (Å)	0.005	0.004
Bond angles (°)	0.699	0.518
Validation		
MolProbity score	1.45	1.6
Clashscore	3.22	5.19
Poor rotamers (%)	0	0
Ramachandran plot[a]		
Favored (%)	95.07	95.32
Allowed (%)	4.93	4.68
Outliers (%)	0	0

[a] Ramachandran plot parameters from PHENIX

Table S2. Table of oligonucleotides, strains, and plasmids

MATERIAL	SOURCE
Oligonucleotides	IDT
sepX top Strand: GTGATATCAGCCAGATCGTGCGACACACCGGGCCAATTGGCCGATGCCGTCCCGCGAAC CCCTCTACCGTGTGAGGCGTGAGCAGCAGCGGCCTCATCGC	
sepX bottom Strand: GCGATGAGGCCGCTGCTGCTCACGCCTCACACGGTAGAGGGGTTCGCGGGACGGCATC GGCCAATTGGCCCGGTGTGTCGCACGATCTGGCTGATATCAC	
sepX-2 top strand: GTGATATCAGCCAGATCGTGCGACACACCGGGCCAATTGGCTTGACACC	
sepX-2 bottom strand: 5'GGTGTCAAGCCAATTGGCCCGGTGTGTCGCACGATCTGGCTGATATCAC	
rpoCfor: CCGGCCAGGCCGTTCCGCTGGAGGACTACGACTACGGTCCGTACAACCAGCATCACCAC CATCACCATTAATTAAATTCCGGGGATCCGTCGACCTGCAG	
rpoCrev: CCGGACACGCCGAAGGGCGGCCACCCCGTGATCGGGGTGACCGCCCTTCGGTCTAAGC GACTCGCTTAATTAATGTAGGCTGGAGCTGCTTCGAAGTTC	
whiAfor TTTATCAAGCTTCGGAGAAACCGAGGGCTTC	
whiArev CTCACTGGTACCTCCGGGGACGGCTCCGGTC	
hrdA_BACTH_F GCTCTAGAGGTGCAGACCCAGTTCGTGTCC	
hrdA_BACTH_R CCGGTACCCGGTCGAGATAGCCGCGCAGCT	
whiB_ BACTH_F CTGAGGATCCCATGACCGAGTTGTTCCAGGAA	
***E. coli* strains**	
E. coli BL21(DE3)	Novagen
E. coli BW25113	Ref (4)
E. coli ET12567 (pUZ8002)	Ref (25)
E. coli BTH101	Ref (26)
***Streptomyces* strains**	
Streptomyces venezuelae NRRL B-65442	Ref (27)
Streptomyces venezuelae AM1	This work
Streptomyces venezuelae whiA SV11	Ref (19)
Recombinant plasmids	
pIJ10754 pCDFDuet-1 plasmid used for co-expression of strep-σ^A/His-WhiB proteins from *Streptomyces venezuelae*	This work
pIJ10755 pSKB2 plasmid derivative used for WhiA protein expression from *Streptomyces venezuelae*	This work
pIJ10757 pET SUMO derivative used for expression of untagged RbpA protein from *Streptomycces venezuelae*	This work
pIJ10762 pCDFDuet-1 plasmid used for co-expression of strep-σ^A protein from *Streptomyces venezuelae*	This work

pIJ773 Plasmid template for amplification of the apr *oriT* cassette for 'Redirect' PCR targeting	Ref (2)
pIJ790 Modified l RED recombination plasmid [*oriR101*] [*repA101*(ts)] *araBp-gam-be-exo*	Ref (2)
pIJ10770 Plasmid cloning vector for the conjugal transfer of DNA from *E. coli* to *Streptomyces* spp. Integrates site specifically at the ΦBT1 attachment site.	Ref(18)
pMB223 *whiB* cloned into BACTH vector pKT25	This work
pIJ10555 pIJ10770 derivative carrying *whiA* expressed from its own promoter to complement the *S. venezuelae whiA* SV11 mutant	This work
pMB657 *whiB* variant sequence encoding WhiB with each of the 4 conserved cysteines substituted for alanine (Cys/Ala) cloned into BACTH vector pKT25	This work
pIJ10922 *sigA* (*hrdB*) cloned into BACTH vector pUT18C	Ref (20)
pIJ10923 *hrdD* cloned into BACTH vector pUT18C	Ref (20)
pMB493 *hrdA* cloned into BACTH vector pUT18C	This work
pMS82 Plasmid cloning vector for the conjugal transfer of DNA from *E. coli* to *Streptomyces* spp. Integrates site specifically at the ΦBT1 attachment site (Hyg^R)	Ref (28)
pIJ10607 pMS82 carrying a mutant version of *whiB* (C25A, C48A, C51A and C57A) expressed from its own promoter	Ref (21)
Pl2 J3 SuperCos1 derivative carrying the *rpoC* region from *Streptomyces venezuelae*	http://strepdb.streptomyces.org.uk/cgi-bin/cosmids.pl?accession=CP018074&width=900
Pl2 J3 *rpoC*-his Pl2 J3 derivative with *rpoC* carrying a C-terminal his tag and marked with an apramycin resistance-*oriT* cassette	This work

237

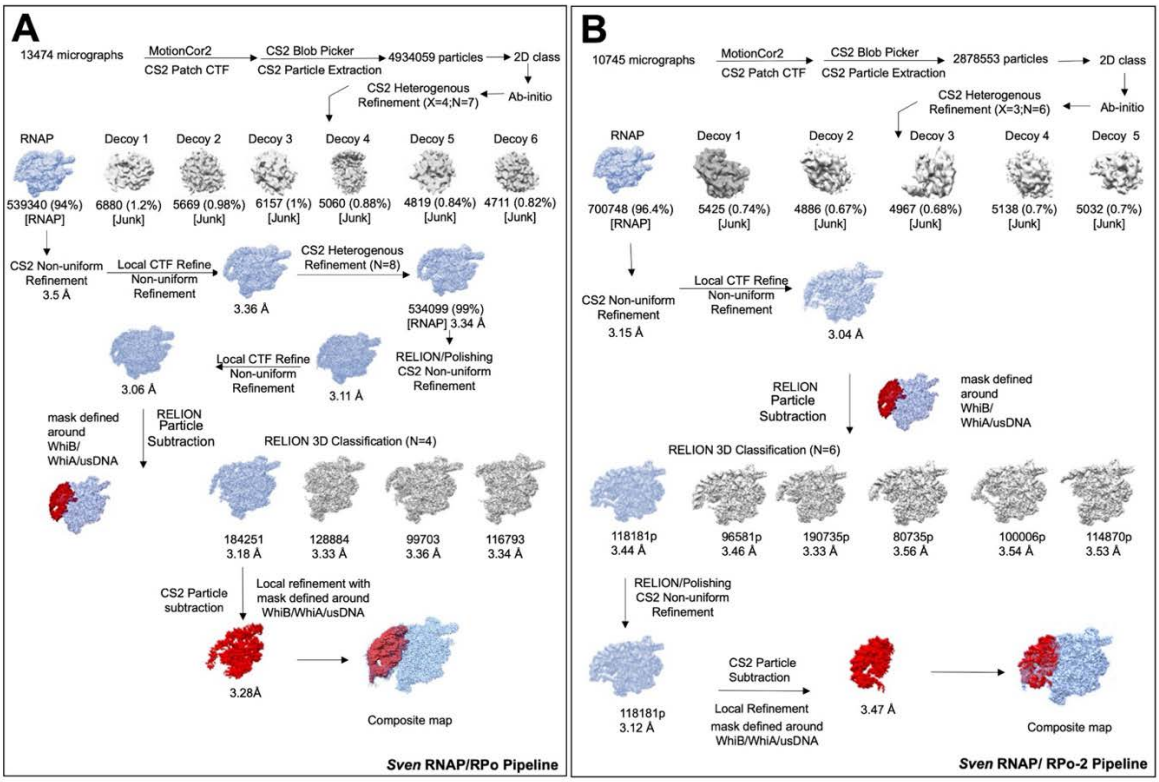

Fig. S1. Data processing workflow for the Sven RNAP/RPo and RPo-2

(A) Flowchart illustrating cryo-EM data processing pipeline for Sven RNAP holoenzyme/WhiA/WhiB/RbpA/*sepX* promoter DNA complex. Dose-fractionated movies (13,474) were frame aligned and summed using MotionCor2 (7). Each micrograph was initially processed in cryoSPARC2 (CS2) (8). The CTF was estimated using Patch CTF; particles were picked using Blob Picker and then extracted. Extracted particles were curated using CS2 Heterogenous Refinement (N=7 classes) using an adaptation of "random-phase 3D classification" (29). Curated particles (blue) were polished in RELION (10, 30) after local CTF refinement in CS2. Polished particles were refined using CS2 Non-uniform Refinement and Local CTF Refinement. They were then classified (N=4) in RELION using signal subtraction (9) masking the region around WhiB, WhiA, alpha-CTD, and the upstream DNA (shown as a red surface). Classified particles were reverted to the non-subtracted particles and refined by CS2 Non-uniform refinement. Particles were then refined by local (BETA) refinement in CS2 with masking the region around WhiB, WhiA, alpha-CTD, and upstream DNA (red mask). A composite map was generated in Phenix from the local refinement RPo map and CS2 non-uniform RPo map and used to generate the final model of RPo.

(B) Flowchart illustrating cryo-EM data processing pipeline for Sven RNAP holoenzyme/WhiA/WhiB/RbpA/sepX-2 promoter DNA complex. Dose-fractionated movies (10,745) were frame aligned and summed using MotionCor2 (7). Each micrograph was initially processed in cryoSPARC2 (CS2) (8). The CTF was estimated using Patch CTF; particles were picked using Blob Picker and then extracted. Extracted particles were curated using CS2 Heterogenous Refinement (N=6 classes) using an adaptation of "random-phase 3D classification" (29). They were then classified (N=4) in RELION using signal subtraction (9) masking the region around WhiB, WhiA, alpha-CTD, and the upstream DNA (shown as a red surface). Classified particles were reverted to the non-subtracted particles and refined by CS2 Non-uniform refinement. Curated particles (blue) were polished in RELION (10, 30) after local CTF refinement in CS2. Polished particles were refined using CS2 Non-uniform

Refinement and Local CTF Refinement. Particles were then refined by local (BETA) refinement in CS2 by masking the region around WhiB, WhiA, alpha-CTD, and upstream DNA (red mask). A composite map was generated in Phenix from the local refinement RPo-2 map and CS2 non-uniform RPo-2 map and used to generate the final model of RPo-2.

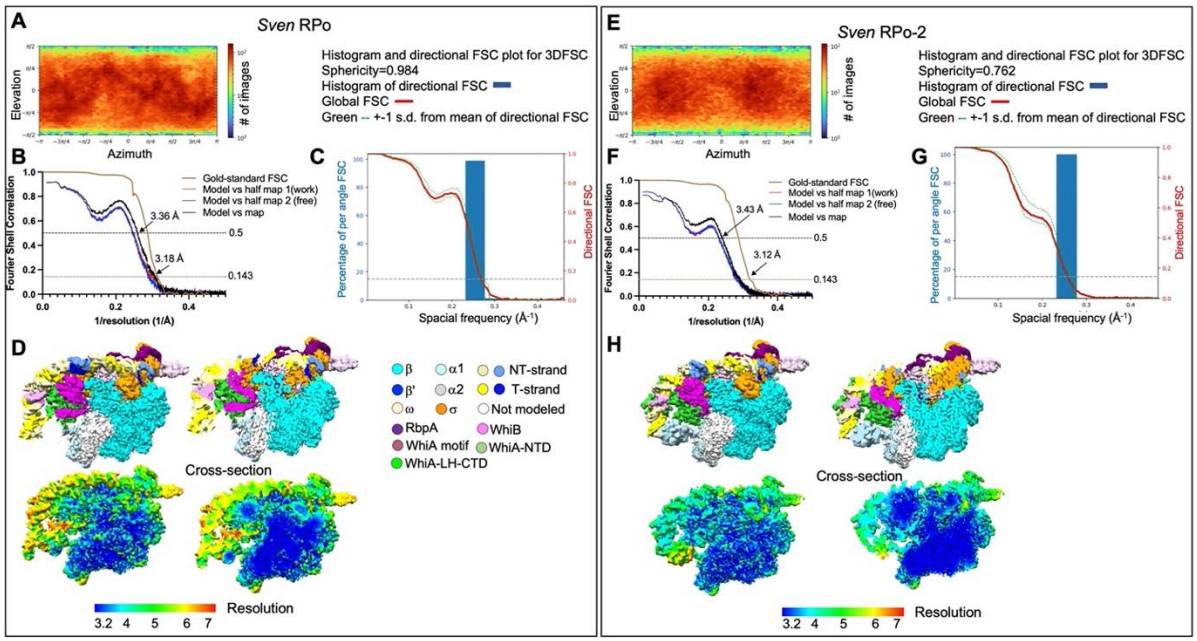

Fig. S2. Analyses and validation of cryo-EM maps

(A) Heat map showing the angular distribution of particle views calculated in cryoSPARC (8) used to calculate the map for *Sven*-RPo.

(B) Gold-standard FSC was calculated from Cryosparc 2 (Punjani *et al.*, 2017) while FSC 0.5 was calculated in phenix.mtriage (12) by providing the combined half maps as well as two independently determined half-maps. The dotted gold line represents the FSC cutoff of 0.143, which indicates a nominal resolution of 3.18 Å. The dotted black line represents the FSC cutoff of 0.5.

(C) Histogram and directional FSC plot of *Sven*-RPo were calculated by 3DFSC (17). Global FSC is represented as a red line.

(D) The cryo-EM density map of *Sven*-RPo is colored according to the key (13). The right view is a cross-section of the left view. The maps below represent local resolution calculations that were generated using blocres from the Bsoft package .

(E) Heat map showing the angular distribution of particle views calculated in cryoSPARC (8) used to calculate the map for *Sven*-RPo-2.

(F) Gold-standard FSC was calculated from Cryosparc 2 and FSC 0.5 was calculated in phenix.mtriage (12) by providing the combined half maps as well as two independently determined half-maps. The dotted gold line represents the FSC cutoff of 0.143, which indicates a nominal resolution of 3.12 Å while the black dotted line represents FSC cutoff of 0.5.

(G) Histogram and directional FSC plot for *Sven*-RPo-2 were calculated by 3DFSC (17). Global FSC is represented as a red line.

(H) The cryo-EM density map of *Sven*RPo-2 is colored according to the key (13). The right view is a cross-section of the left view. The maps below represent local resolution calculations that were generated using blocres from the Bsoft package (13)

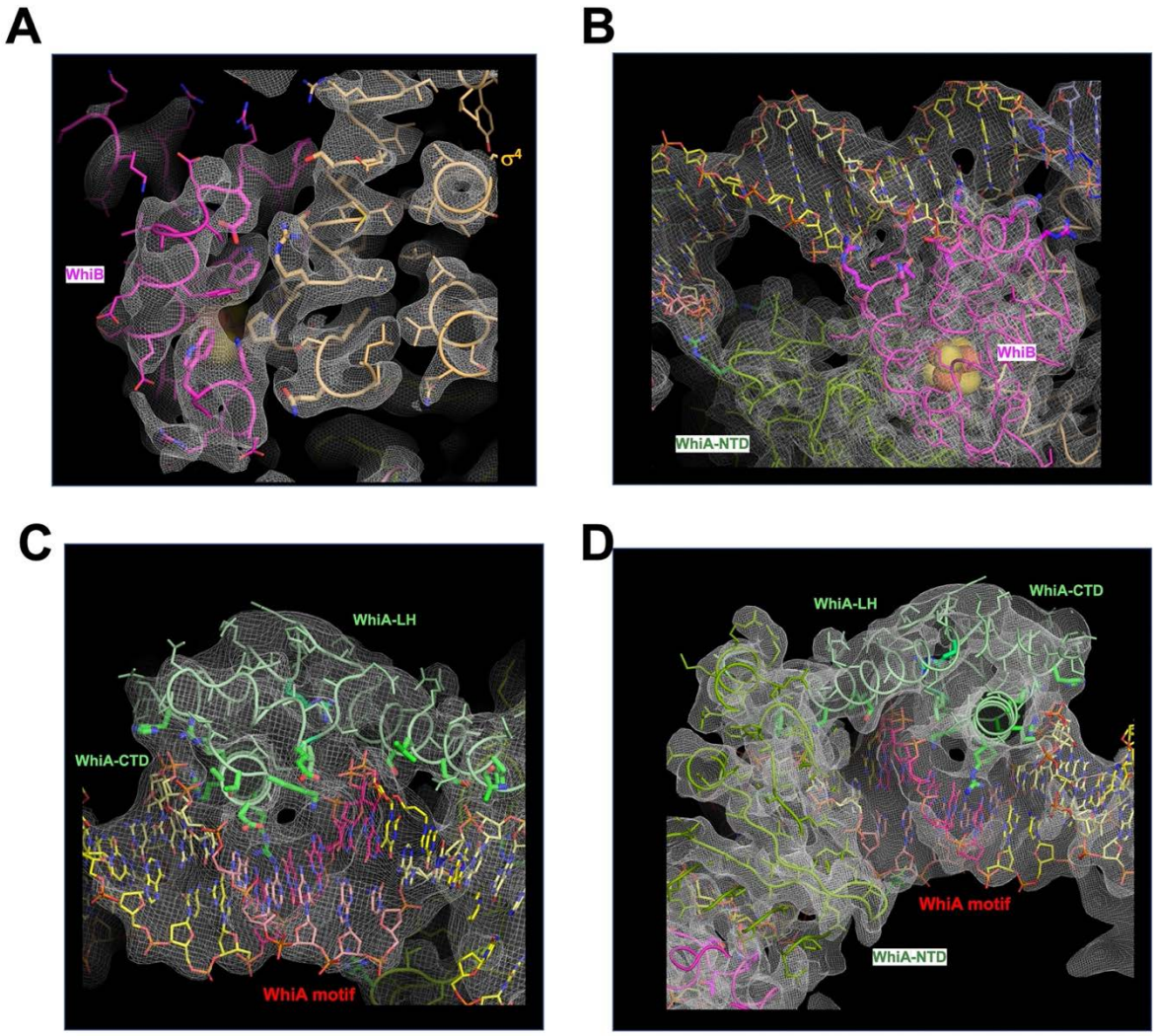

293

294 **Fig. S3. Cryo-EM density map of WhiA and WhiB interactions**

295 (A) Density map of the interface between WhiB and σ^{A}_{4}.

296 (B) Density map of the interface between and WhiB and the DNA and WhiA-NTD and the DNA.

297 (C) Density map of the interface between WhiA-CTD and the WhiA motif.

298 (D) Density map of the interface between WhiA-CTD and the WhiA motif; view is turn 180^{o} around the
299 x-axis to (C).

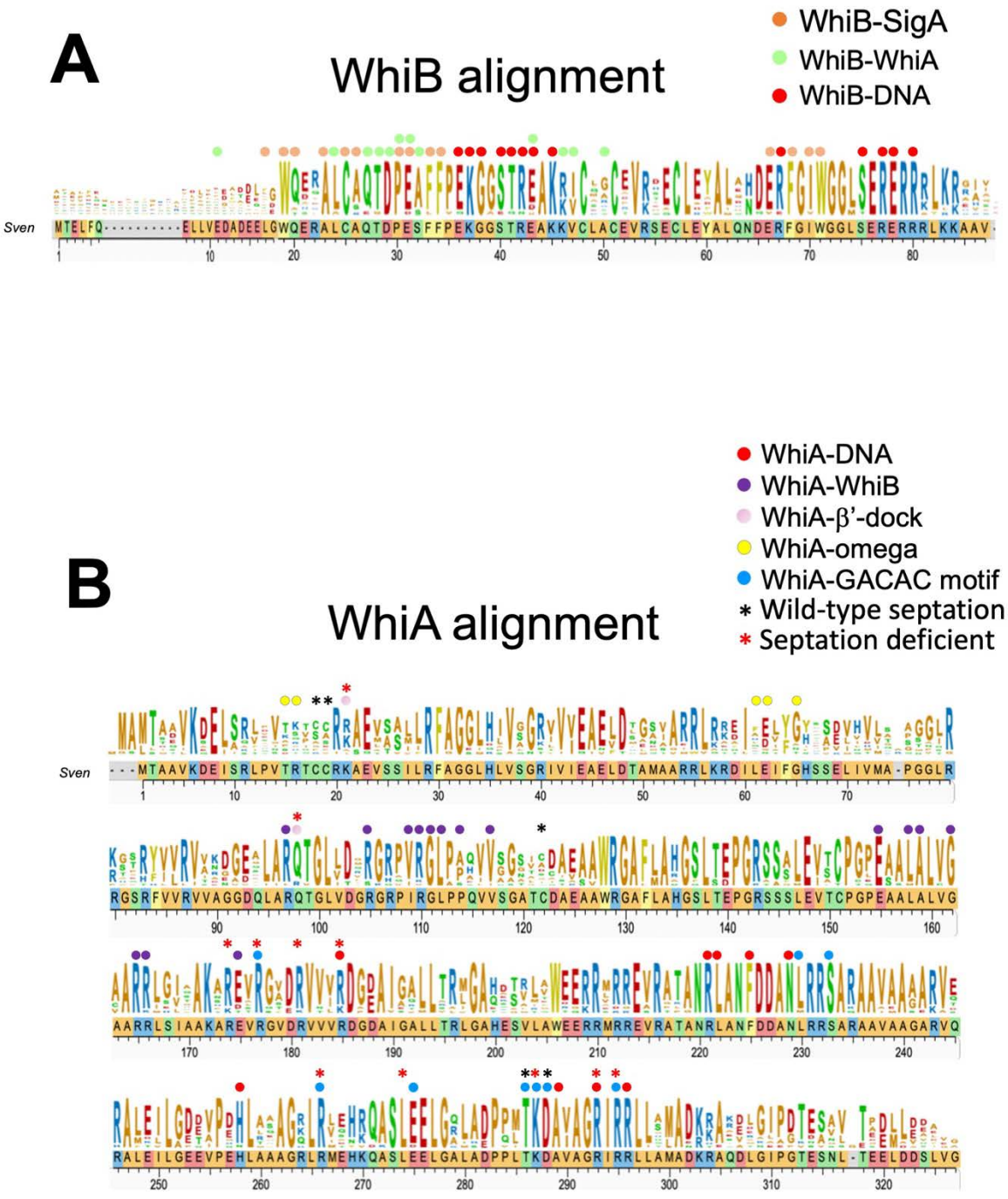

Fig. S4. Conservation of interacting residues of WhiA and WhiB

(A) Sequence of *Sven* WhiB with Seq-logo above. This logo is derived from the alignment of WhiB from *Streptomyces venezuelae*, *Streptomyces coelicolor*, *Mycobacterium tuberculosis*, *Mycobacterium bovis*, *Mycobacterium leprae*, *Corynebacterium glutamicum*, *Corynebacterium diphtheriae*, *Stackebrandtia nassauensis*, *Salinispora tropica*, *Saccharopolyspora erythraea*, *Micromonospora sp*, *Amycolatopsis mediterranei*, *Gordonia bronchialis*, *Nocardia farcinica*, *Rhodococcus jostii*, *Nocardioides sp*, *Kineococcus radiotolerans*, *Micrococcus luteus*, and *Bifidobacterium longum*. Residues of WhiB interacting with SigA are labeled as orange dots. WhiB residues interacting with WhiA are labeled as green residues. WhiB residues interacting with DNA are labeled as red dots. The alignment shows that most of the residues of WhiB that interact with σ^A are conserved. Alignments and

seq-logo for (A) and (B) were generated by Megalign Pro (DNASTAR). Alignment is provided in supplemental datafile 2 and complete list of contacts in supplemental datafile 1.

(B) Sequence of *Sven* WhiA. The above alignment is a Seq-logo derived from alignment with WhiA from representative Actinobacteria listed above for WhiB alignment. Red dots indicate WhiA_DNA interactions. Purple dots indicate WhiA-WhiB interactions. Pink dots indicate WhiA-β' dock interactions. Yellow dots indicate WhiA-ω interactions. WhiA-WhiA consensus sequence motif (GACAC) interactions are displayed as blue dots. Red and black asterisks indicate mutations that did or did not lead to a sporulation division defect, respectively. The alignment shows that residues of WhiA that interact with the WhiA motif are conserved. Alignment is provided in supplemental datafile 3 and complete list of contacts in supplemental datafile1.

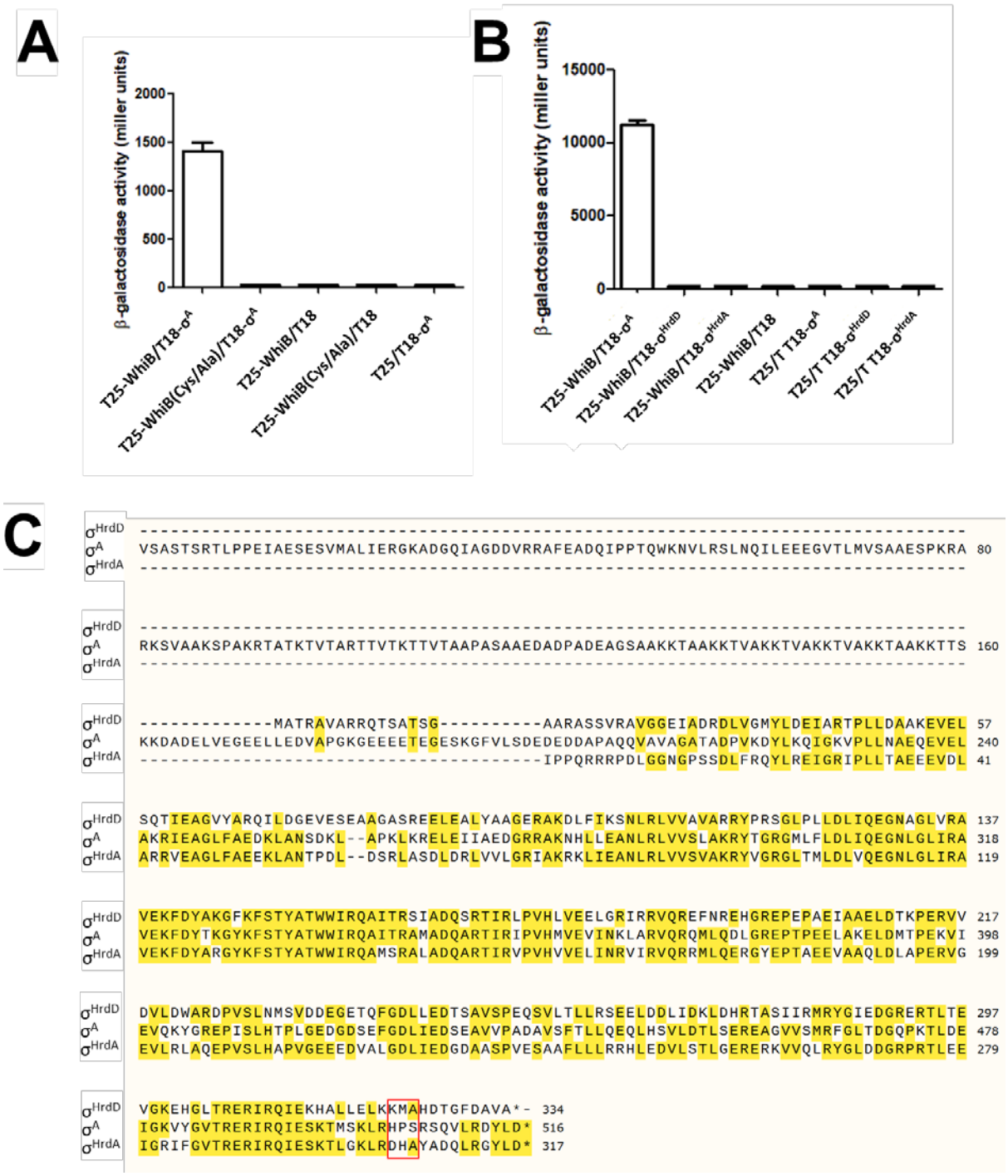

Fig. S5. WhiB interacts specifically with the primary housekeeping sigma factor, σ^A, and this interaction requires the WhiB [4Fe-4S] cluster

(A) WhiB but not the WhiB 4Cys→4Ala variant that lacks the [4Fe-4S] cluster interacts with σ^A in an *E. coli* bacterial adenylate cyclase two-hybrid (BACTH) assay.

(B) WhiB interacts with the primary housekeeping sigma factor, σ^A, but not with the related Group I sigma factors σ^{HrdA} or σ^{HrdD} in the same *E. coli* BACTH assay. β-galactosidase activities resulting from the interaction between T25 and T18 N-terminal fusions are shown as the average of three biological replicates, with error bars showing the standard error of the mean. The results from negative control

experiments measuring interaction with the individual T25 and T18 fragments of adenylate cyclase are also shown.

(C) Protein sequence alignment of the primary housekeeping sigma factor σ^{A} with the two other Group I sigma factors found in *S. venezuelae*, σ^{HrdA} and σ^{HrdD}. Conserved residues are highlighting in yellow. The His-Pro-Ser motif that is present in σ^{A} but not in σ^{HrdD} and σ^{HrdA} is boxed in red. The cryo-EM structure shows that this His-Pro-Ser motif in σ^{A} interacts directly with the WhiB [4Fe-4S] cluster.

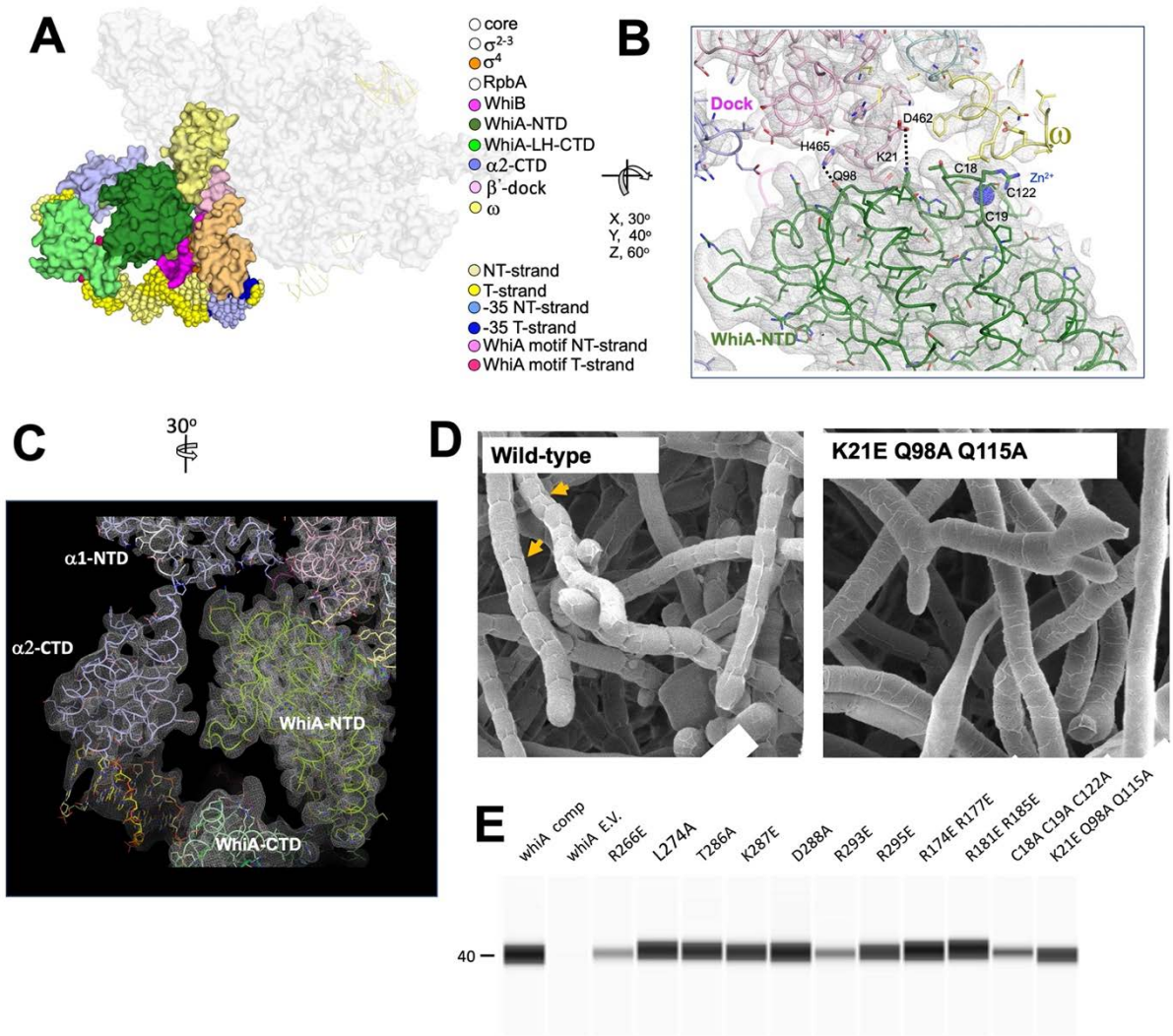

Fig. S6. WhiA-NTD interactions with RNAP

(A) Upstream protein-protein and protein-DNA interactions of the WhiA/WhiB/RNAP initiation complex. The α2-CTD, WhiA, WhiB, the dock, ω and $\sigma^{A}{}_{4}$, are shown in solid colored surface; the rest of RNAP is in semi-transparent light gray. The upstream promoter DNA is rendered in spheres.

(B) Density map of the interface between WhiA-NTD and the dock and ω.

(C) Density map of the interface between α-CTD and the upstream DNA and WhiA-NTD.

(D) Scanning Electron Micrographs showing that mutating three residues in the WhiA-NTD that sit at the interface with the β'-dock domain (K21E, Q98A, and Q115A) abolishes developmental cell division. Representative sporulation septa in the wild-type strain are indicated by orange arrows.

(E) Automated WhiA Western blot analysis of the strains shown in Figures 6B and S6D, generated using the quantitative 'Wes' capillary electrophoresis and blotting system (ProteinSimple – San Jose, CA; see Methods).

SI References

1. A. Morin, *et al.*, Collaboration gets the most out of software. *eLife* **2**, e01456 (2013).

2. B. Gust, G. L. Challis, K. Fowler, T. Kieser, K. F. Chater, PCR-targeted *Streptomyces* gene replacement identifies a protein domain needed for biosynthesis of the sesquiterpene soil odor geosmin. *Proc. Natl. Acad. Sci. U.S.A.* **100**, 1541–1546 (2003).

3. B. Gust, *et al.*, "λ Red-Mediated Genetic Manipulation of Antibiotic-Producing *Streptomyces*" in *Advances in Applied Microbiology*, (Elsevier, 2004), pp. 107–128.

4. K. A. Datsenko, B. L. Wanner, One-step inactivation of chromosomal genes in *Escherichia coli* K-12 using PCR products. *Proc. Natl. Acad. Sci. U.S.A.* **97**, 6640–6645 (2000).

5. C. A. Schneider, W. S. Rasband, K. W. Eliceiri, NIH Image to ImageJ: 25 years of image analysis. *Nature Methods* **9**, 671–675 (2012).

6. W. V. Nicholson, H. White, J. Trinick, An approach to automated acquisition of cryoEM images from lacey carbon grids. *Journal of Structural Biology* **172**, 395–399 (2010).

7. S. Q. Zheng, *et al.*, MotionCor2: Anisotropic correction of beam-induced motion for improved cryo-electron microscopy. *Nature Methods* **14**, 331–332 (2017).

8. A. Punjani, J. L. Rubinstein, D. J. Fleet, M. A. Brubaker, CryoSPARC: Algorithms for rapid unsupervised cryo-EM structure determination. *Nature Methods* **14**, 290–296 (2017).

9. X. Bai, E. Rajendra, G. Yang, Y. Shi, S. H. Scheres, Sampling the conformational space of the catalytic subunit of human γ-secretase. *eLife* **4**, e11182 (2015).

10. S. H. W. Scheres, RELION: Implementation of a Bayesian approach to cryo-EM structure determination. *J Struct Biol* **180**, 519–530 (2012).

11. P. D. Adams, *et al.*, PHENIX: A comprehensive Python-based system for macromolecular structure solution. *Acta Crystallographica Section D: Biological Crystallography* **66**, 213–221 (2010).

12. P. V. Afonine, *et al.*, New tools for the analysis and validation of cryo-EM maps and atomic models. *Acta Crystallogr D Struct Biol* **74**, 814–840 (2018).

13. G. Cardone, J. B. Heymann, A. C. Steven, One number does not fit all: Mapping local variations in resolution in cryo-EM reconstructions. *Journal of Structural Biology* **184**, 226–236 (2013).

14. M. Lilic, S. A. Darst, E. A. Campbell, Structural basis of transcriptional activation by the *Mycobacterium tuberculosis* intrinsic antibiotic-resistance transcription factor WhiB7. *Molecular Cell* **81**, 2875-2886.e5 (2021).

15. E. F. Pettersen, *et al.*, UCSF Chimera?A visualization system for exploratory research and analysis. *J. Comput. Chem.* **25**, 1605–1612 (2004).

16. P. Emsley, K. Cowtan, Coot: Model-building tools for molecular graphics. *Acta Crystallographica Section D: Biological Crystallography* **60**, 2126–2132 (2004).

17. Y. Z. Tan, *et al.*, Addressing preferred specimen orientation in single-particle cryo-EM through tilting. *Nat Methods* **14**, 793–796 (2017).

18. S. Schlimpert, *et al.*, Two dynamin-like proteins stabilize FtsZ rings during *Streptomyces* sporulation. *Proc. Natl. Acad. Sci. U.S.A.* **114** (2017).

19. M. J. Bush, M. J. Bibb, G. Chandra, K. C. Findlay, M. J. Buttner, Genes Required for Aerial Growth, Cell Division, and Chromosome Segregation Are Targets of WhiA before Sporulation in *Streptomyces venezuelae. mBio* **4**, e00684-13 (2013).

20. M. Y. Y. Stewart, M. J. Bush, J. C. Crack, M. J. Buttner, N. E. Le Brun, Interaction of the *Streptomyces* Wbl protein WhiD with the principal sigma factor σ^{HrdB} depends on the WhiD [4Fe-4S] cluster. *Journal of Biological Chemistry* **295**, 9752–9765 (2020).

21. M. J. Bush, G. Chandra, M. J. Bibb, K. C. Findlay, M. J. Buttner, Genome-Wide Chromatin Immunoprecipitation Sequencing Analysis Shows that WhiB Is a Transcription Factor That Cocontrols Its Regulon with WhiA To Initiate Developmental Cell Division in *Streptomyces*. *mBio* **7**, e00523-16 (2016).

22. M. M. Al-Bassam, M. J. Bibb, M. J. Bush, G. Chandra, M. J. Buttner, Response Regulator Heterodimer Formation Controls a Key Stage in *Streptomyces* Development. *PLoS Genet* **10**, e1004554 (2014).

23. M. J. Bibb, Á. Domonkos, G. Chandra, M. J. Buttner, Expression of the chaplin and rodlin hydrophobic sheath proteins in *Streptomyces venezuelae* is controlled by σ^{BldN} and a cognate anti-sigma factor, RsbN: Regulation of the chaplin genes in *Streptomyces*. *Molecular Microbiology* **84**, 1033–1049 (2012).

24. J. H. Miller, *Experiments in molecular genetics* (Cold Spring Harbor Laboratory, 1972).

25. M. S. B. Paget, L. Chamberlin, A. Atrih, S. J. Foster, M. J. Buttner, Evidence that the Extracytoplasmic Function Sigma Factor σ^{E} Is Required for Normal Cell Wall Structure in *Streptomyces coelicolor* A3(2). *J Bacteriol* **181**, 204–211 (1999).

26. G. Karimova, J. Pidoux, A. Ullmann, D. Ladant, A bacterial two-hybrid system based on a reconstituted signal transduction pathway. *Proc. Natl. Acad. Sci. U.S.A.* **95**, 5752–5756 (1998).

27. J. P. Gomez-Escribano, *et al.*, *Streptomyces venezuelae* NRRL B-65442: genome sequence of a model strain used to study morphological differentiation in filamentous actinobacteria. *Journal of Industrial Microbiology and Biotechnology* **48**, kuab035 (2021).

28. M. A. Gregory, R. Till, M. C. M. Smith, Integration Site for *Streptomyces* Phage φBT1 and Development of Site-Specific Integrating Vectors. *J Bacteriol* **185**, 5320–5323 (2003).

29. X. Gong, *et al.*, Structural Insights into the Niemann-Pick C1 (NPC1)-Mediated Cholesterol Transfer and Ebola Infection. *Cell* **165**, 1467–1478 (2016).

30. J. Zivanov, *et al.*, New tools for automated high-resolution cryo-EM structure determination in RELION-3. *eLife* **7**, e42166 (2018).